Design and Preliminary Evaluation of a Hybrid Electromagnetic Suspension Test Rig for an Automotive Vibration Isolator

Pandher, C.S.[a,*]; Farwaha, H.S.[a]; Deepak, D.[b]

[a] Department of Mechanical and Production Engineering, Guru Nanak Dev Engineering College, Ludhiana, Punjab, India
[b] Department of Mechanical Engineering, Punjabi University, Patiala, Punjab, India

ABSTRACT
This paper describes the design, fabrication and preliminary evaluation of a hybrid electromagnetic suspension test rig for automotive vibration isolation and shock absorption. The work was developed from a research work involving a retrofit electromagnetic suspension concept, a vehicle-based test rig, computer-aided design (CAD) modelling, structural analysis and fabrication. The proposed arrangement combines electromagnetic forces with conventional suspension components. Permanent magnets and electromagnets are used to produce repulsive or controllable forces, while a spring and hydraulic damper provide mechanical support and damping. The procedure included measurement of an actual vehicle suspension, CAD development, preparation of alternative test-rig designs, structural analysis, fabrication and functional checking. The second test-rig design was selected because it required less material, was easier to fabricate and included a protective upper cover. The reported structural analysis used a 3 mm mild-steel structure and a load of 783.96 N, giving calculated displacements of 0.00126 mm for the lower section and 0.0007 mm for the upper section. For the electromagnetic actuator, the reported calculation used 1150 turns, a 0.1 m coil length, relative permeability of 200 and a current of 4 A, giving an estimated magnetic flux density of about 11.55 T and force of 4.62 N. The fabricated rig accommodated the spring, damper and electromagnetic unit and showed the intended basic movement. The work provides a laboratory platform for future studies using sensors, improved magnetic circuits and lighter structural materials.

Keywords: Automotive suspension; vibration isolation; electromagnetic suspension; electromagnetic actuator; test rig

Corresponding author: Pandher, C.S. — Department of Mechanical and Production Engineering, Guru Nanak Dev Engineering College, Ludhiana, Punjab, India. E-mail: chatwant@gndec.ac.in

1. Introduction

An automotive suspension must control the transmission of road disturbances to the vehicle body while maintaining adequate tyre contact with the road. In a conventional passive suspension, the spring stores and releases mechanical energy and the damper dissipates vibration energy (Fu *et al.*, 2023). The project considered whether part of the energy normally dissipated during suspension motion could instead be used for electromagnetic assistance or energy recovery, particularly for hybrid and electric vehicles.

Electromagnetic forces can be incorporated into suspension systems in different ways. An electromagnetic actuator can provide a controllable force or an equivalent spring effect, while the relative movement of magnets and coils can also be used for energy conversion (Gysen *et al.*, 2011; Fu *et al.*, 2023). The approach followed in the project is retrofit-based: an electromagnetic unit is added to an existing suspension rather than replacing the complete assembly. This allows the conventional mechanical components to remain in service while an electrically controlled function is added.

The project examines two related arrangements. The first is a retrofit electromagnetic/regenerative unit in which a coil and magnet interact during relative motion. The second is an electromagnetic shock absorber using electromagnets, permanent magnets, a spring, push rods and a direct-current (DC) supply, with polyvinyl chloride (PVC) components in the proposed assembly. A separate test rig was built around a vehicle spring and damper to provide a practical arrangement for examining the electromagnetic system. The retrofit assembly is illustrated in Fig. 1.

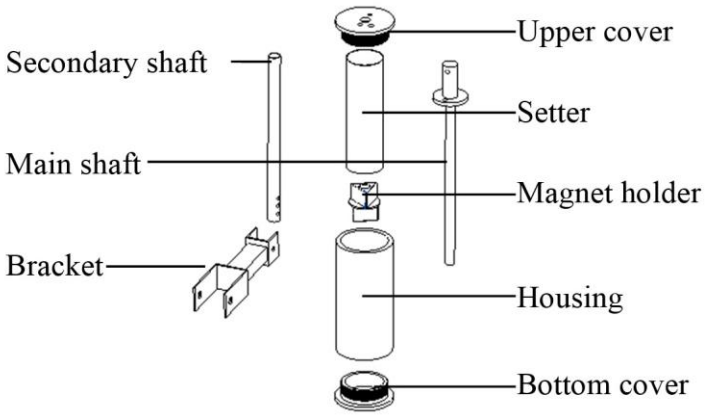


Fig. 1 Exploded view of the retrofit electromagnetic suspension system (Gysen *et al.*, 2009; Gysen *et al.*, 2010).

2. Literature review and research gap

Research on electromagnetic suspension has progressed from magnetic-suspension principles to active control, permanent-magnet actuators and regenerative arrangements. The following synthesis presents these developments chronologically and identifies the practical gap addressed by the present study.

Danby and Powell (1966) introduced an electrodynamic-suspension concept for high-speed transportation. Later automotive studies addressed fuzzy and adaptive-fuzzy control (Sharkawy, 2005) and robust linear control evaluated on a quarter-car test rig (Lauwerys *et al.*, 2005). Paulides *et al.* (2006) examined semi-active electromagnetic-suspension design, while Martins *et al.* (2006) assessed the applicability of permanent-magnet linear actuators.

Actuator research subsequently compared linear permanent-magnet motor topologies (Wang *et al.*, 2008). Gysen *et al.* (2009, 2010, 2011) investigated a tubular permanent-magnet actuator combined with a passive spring, improvements in vehicle dynamics and the efficiency of regenerative direct-drive actuation, respectively. Related work examined the design and characterisation of an electromagnetic suspension energy harvester (Zuo *et al.*, 2010).

An industrial electromagnetic active-suspension concept was described by Bose Corporation (2011). Li *et al.* (2013) studied energy-harvesting shock absorbers using design, modelling and road tests. Abdelkareem *et al.* (2018) reviewed vibration energy harvesting in vehicle suspensions, and Zhang *et al.* (2020) compared energy-harvesting predictions from quarter-, half- and full-vehicle models.

Reviews and development studies published in 2023 addressed electromagnetic energy-regenerative suspension technologies and their key design issues (Fu *et al.*, 2023), energy harvesting through suspension systems (Tulsian and Dewangan, 2023), and the development of a regenerative shock absorber (Dahat *et al.*, 2023).

Studies published in 2024 expanded the emphasis to active control and energy-efficient design. Shi *et al.* (2024) investigated a self-powered, dual-function active electromagnetic damper, while Puliti *et al.* (2024) formulated a multi-objective optimisation approach for regenerative shock absorbers. Wu *et al.* (2024) explored the effect of time delay on energy recovery, and Yang and Cen (2024) analysed stochastic suspension dynamics with delayed feedback and fractional damping.

More recent work encompasses linear-motor technologies (Sun *et al.*, 2025), optimisation of an integrated electromagnetic linear regenerative suspension (Lu *et al.*, 2025), and energy-recovery control in a hybrid electric-vehicle suspension (Xing *et al.*, 2025). Liu *et al.* (2025) examined an electromagnetic–hydraulically interconnected suspension through modelling, bench testing and ride analysis. Xiong *et al.* (2025) investigated energy harvesting using Halbach-like magnet arrays, and Ding *et al.* (2026) reviewed linear-motor suspension configurations and control strategies.

Research gap and relevance to the present study. The cited work offers actuator concepts, control approaches, energy-recovery studies and several forms of experimental validation. The

present study addresses a narrower practical requirement: documenting a laboratory test-rig development sequence that connects measurements of an actual vehicle suspension, alternative computer-aided design (CAD) configurations, structural assessment, fabrication and preliminary functional checking of a combined spring–damper and electromagnetic arrangement. The contribution is this integrated design-and-fabrication assessment; dynamic suspension performance and energy recovery have not yet been experimentally validated on the fabricated rig.

3. Problem formulation

The work investigates an alternative suspension arrangement in which electromagnetic force is added without removing the practical functions of the conventional spring and damper. The project also identifies engineering issues such as design complexity, robustness, magnetic leakage, manufacturability and controlled movement of the moving parts. Related actuator design considerations are discussed in (Gysen *et al.*, 2009).

Stability is another important issue. Magnetic force alone may not keep the moving member on the required path. The proposed arrangement therefore retains mechanical guidance and hydraulic damping, with provision for position sensing and controlled electromagnet operation. The spring and damper are not removed; instead, electromagnetic force is introduced as an additional controllable element. A published direct-drive configuration similarly combines electromagnetic actuation with a passive spring and damper (Gysen *et al.*, 2011).

The main task is to design and fabricate a practical electromagnetic suspension/shock-absorber arrangement together with a safe laboratory test rig. The rig must support a vehicle spring and damper and provide a suitable platform for examining electromagnetic force, structural response and suspension movement.

4. Objectives and research contribution

- To develop an electromagnetic suspension concept suitable for automotive shock absorption and vibration isolation.
- To study the use of electromagnetic and permanent-magnet forces in a suspension arrangement.
- To obtain the dimensions and geometry of an actual vehicle suspension configuration and reproduce the relevant arrangement in a laboratory test rig.
- To develop alternative CAD models for the test rig and select a configuration considering safety, manufacturability and material requirement.
- To perform structural/stress analysis of the selected test-rig design under the reported loading condition.
- To fabricate the test rig using practical workshop processes and integrate the spring, damper and electromagnetic subsystem.
- To evaluate the basic functional movement of the fabricated assembly and identify future improvements involving sensors, magnets and lightweight materials.

Research contribution: The main contribution of this study is the development and fabrication of a vehicle-representative laboratory test rig integrating a conventional spring–damper assembly with an electromagnetic actuation subsystem. The study links measured vehicle geometry, CAD design, structural assessment, fabrication and preliminary functional evaluation in a single experimental platform.

5. System architecture and working principle

The proposed arrangement adds electromagnetic actuation to a conventional mechanical suspension. In the configuration described in the project, an electromagnetic cylinder and cylindrical magnets are positioned with like poles facing one another to produce repulsion. Damping can be provided by a hydraulic damper, while an alternative arrangement uses a linear electromag-

netic motor in place of the conventional damping element. Linear-motor and hydraulic-electric suspension architectures are reviewed in (Fu *et al.*, 2023). The feedback principle is illustrated in Fig. 2.

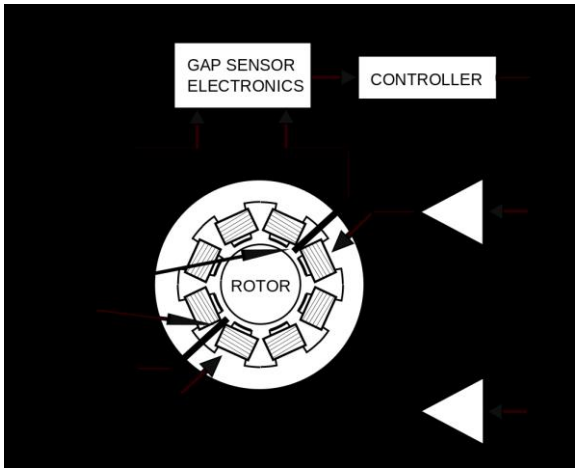


Fig. 2 Basic feedback-oriented electromagnetic suspension principle shown in the source report (Gysen *et al.*, 2009; Gysen *et al.*, 2010).

In a feedback-controlled arrangement, gap sensors provide the position of the moving member. The measured position can be compared with a reference value, and the controller can then adjust the current supplied to the electromagnets through the power electronics. The vehicle-level concept similarly relates suspension stiffness, electromagnetic actuation, level sensing and motor control (Gysen *et al.*, 2009; Fu *et al.*, 2023). The vehicle-level architecture is summarised in Fig. 3.

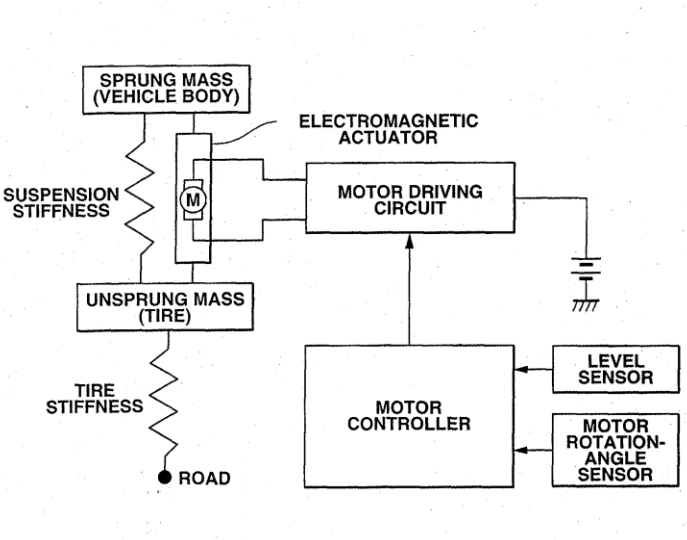


Fig. 3 Vehicle-level electromagnetic suspension block diagram (Gysen *et al.*, 2010).

Two shock-absorber arrangements are considered. The first combines magnetic repulsion with a hydraulic damper. The second uses a linear electromagnetic motor instead of the conventional damping element. Electrical control of the actuator allows the applied force to be changed rapidly in response to wheel disturbances (Gysen *et al.*, 2009; Gysen *et al.*, 2010). Table 1 summarises the components and their functions.

Table 1 Components and functions of the hybrid suspension system

Subsystem	Main components identified in source	Function
Mechanical support	Support mounting, spring, cylinder, piston/push rods	Carries and guides suspension motion.
Magnetic subsystem	Permanent magnets / electromagnets	Generates repulsive or controllable electromagnetic force.
Damping subsystem	Hydraulic damper or linear electromagnetic motor	Controls oscillatory motion and shock response.
Electrical subsystem	DC supply/battery, electromagnet, inverter/power electronics	Provides controlled electrical energy.
Guidance and safety	Shaft, housing, protective cover	Restrains unstable motion and protects the operator.

6. Test-rig design and experimental methodology

6.1 Methodology flow

Table 2 outlines the sequence used to design, fabricate and check the test rig.

Table 2 Methodology stages for design and fabrication of the test rig

Stage	Activity	Output
1	Collect data from previous suspension systems and direct observation	Design requirements and reference geometry
2	Measure real vehicle suspension dimensions	Spring/damper position and angles
3	Select materials and process parameters	Preliminary design inputs
4	Develop CAD models and alternative test-rig configurations	Candidate designs
5	Analyse selected suspension/test-rig configuration	Structural response
6	Optimise design for safety and manufacturability	Final test-rig design
7	Fabricate structural components	Physical test rig
8	Assemble spring, damper and electromagnetic subsystem	Integrated test setup
9	Test individual and assembled components	Functional verification
10	Collect and interpret observations	Design conclusions and future improvements

6.2 Dimensional measurement and CAD development

The test-rig dimensions were taken from a disassembled vehicle suspension. A Vernier calliper and ruler were used for the main measurements, including spring and damper locations, and the relevant component angles were recorded. The measured suspension is shown in Fig. 4.

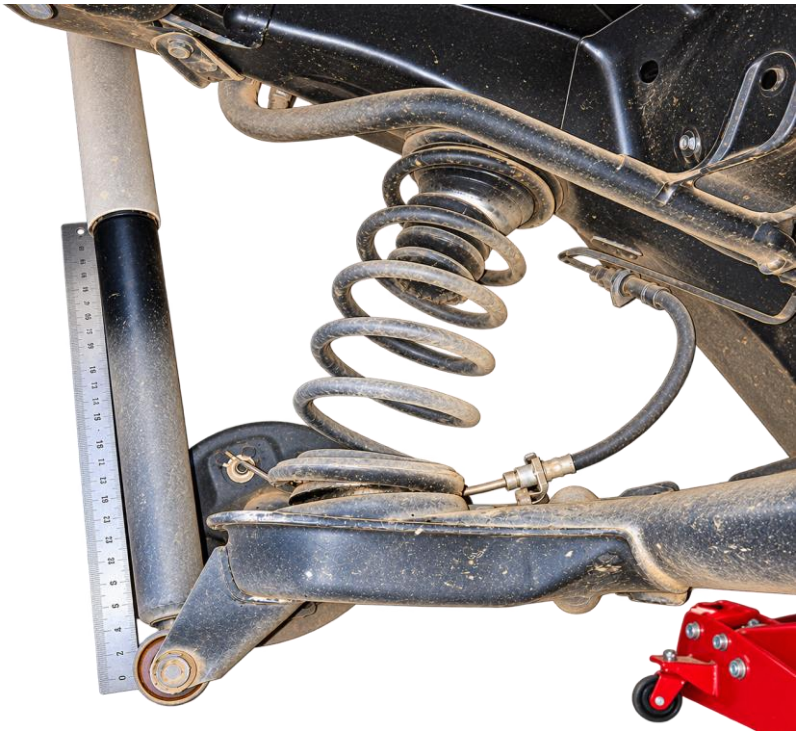


Fig. 4 Measurement of the real vehicle suspension

The measured suspension geometry was transferred into a CAD model and combined with the proposed test-rig structure. Two designs were prepared. The first was more complicated and did not include a protective cover. The second had a simpler structure, required less material and included an upper protective cover. The two candidate designs are shown in Fig. 5 and Fig. 6.

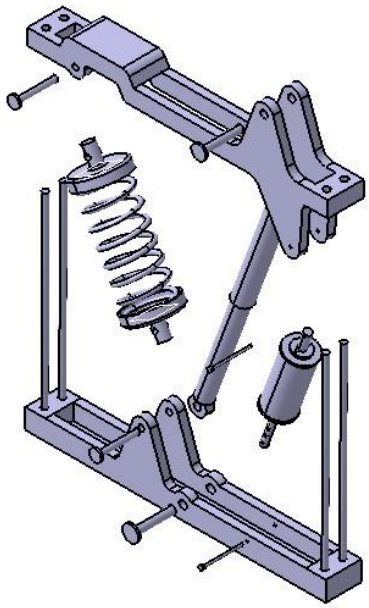


Fig. 5 First test-rig CAD design; project CAD model. Related electromagnetic actuator design studies: (Paulides *et al.*, 2006; Gysen *et al.*, 2009).

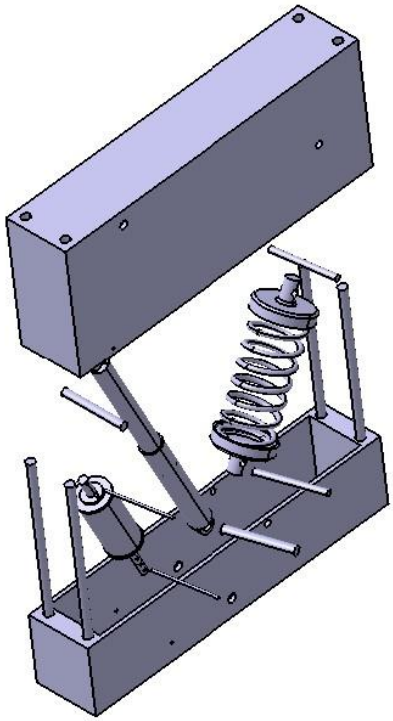


Fig. 6 Second test-rig CAD design with protective upper cover; project CAD model. Related electromagnetic actuator design studies: (Paulides *et al.*, 2006; Gysen *et al.*, 2009).

6.3 Selection of the test-rig design

The second configuration was selected for fabrication because it was simpler to manufacture and required less material. The upper protective plate also provides an additional barrier if a fastener or component becomes loose during testing. These features made the second design more suitable for laboratory use. Table 3 compares the two designs.

Table 3 Comparison of alternative test-rig designs

Criterion	**First design**	**Second design / selected configuration**
Geometry	More complex	Simplified
Safety	No upper protective cover	Upper cover provided
Fabrication	More processes	Reduced fabrication complexity
Material requirement	Higher	Lower
Suitability for laboratory use	Less convenient	Selected for fabrication

6.4 Structural analysis

Before fabrication, the selected design was checked through structural analysis. A 3 mm mild-steel sheet was selected for the rig as a practical material for the required load and workshop fabrication. For the reported load of 783.96 N, the calculated displacement was 0.00126 mm in the lower section and 0.0007 mm in the upper section. Table 4 summarises the structural inputs and results.

Table 4 Structural-analysis parameters and reported results

Parameter	Source-reported value	Interpretation
Test-rig material	Mild steel	Selected for load carrying capability and low fabrication cost.
Structural thickness	3 mm	Sheet thickness used for fabrication.
Applied force	783.96 N	Load used in the reported structural analysis.
Lower-part displacement	0.00126 mm	Very small reported deformation under the analyzed load.
Upper-part displacement	0.0007 mm	Very small reported deformation under the analyzed load.

6.5 Fabrication procedure

The physical test rig was made from 3 mm mild-steel sheet. The individual members were cut, sheared and bent and then welded together. The spring, damper and retrofit electromagnetic regenerative unit were subsequently installed on the fabricated structure. The fabricated assembly is shown in Fig. 7.



Fig. 7 Complete fabricated test rig

The completed rig accommodated the main suspension components, and its movement was checked during a practical trial. The reported observation confirms basic mechanical operation of the assembly. It should not be considered a full vehicle-level ride or dynamic-performance test. Published suspension studies use quarter-car measurements to validate actuator and control performance (Gysen *et al.*, 2009; Gysen *et al.*, 2011).

7. Electromagnetic actuator and hybrid suspension design

The proposed electromagnetic shock absorber consists of two electromagnets, two permanent magnets, two movable push rods, a DC source, a steel-wire spring and PVC pipe elements. The push rods guide the moving parts in a manner similar to piston rods. During displacement, the magnetic interaction produces a restoring force that contributes to the suspension response.

The project also considers a hybrid arrangement in which two magnets are guided by a shaft while a hydraulic damper is retained. The magnets are placed with like poles facing each other to

produce repulsion, and the shaft limits lateral movement. The hydraulic damper absorbs part of the vibration and helps prevent excessive oscillation. Mechanical guidance is therefore retained when magnetic repulsion is used. The hydraulic damper is shown in Fig. 8.

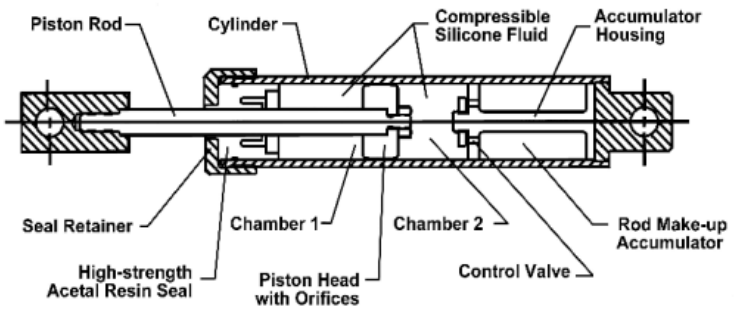


Fig. 8 Hydraulic damper schematic (Abdelkareem *et al.*, 2018).

Another arrangement uses a linear electromagnetic motor. Interaction between the coils and magnets produces controlled extension and retraction. Electrical actuation can respond quickly to wheel disturbances and may also be used to address body roll and pitch (Gysen *et al.*, 2009). The project further considers a regenerative power amplifier for returning part of the energy associated with compression to the electrical system. The combination of active-force production and regenerative operation has been analysed and tested in a direct-drive suspension (Gysen *et al.*, 2011).

8. Electromagnetic and structural calculations

The actuator calculations distinguish between the specified design inputs and the quantities obtained from the equations. The numerical values used below are those reported in the project report. Table 5 lists the design inputs, and Table 6 lists the calculated outputs.

Table 5 Input parameters for electromagnetic actuator design

Input parameter	**Value**	**Unit**	**Basis**
Relative permeability factor, K	200	Dimensionless	Given
Permeability of free space, μ_0	$4\pi \times 10^{-7}$	H/m	Constant used in calculation
Number of turns, N	1150	turns	Given
Coil length, L	0.10	m	Given
DC current, I	4	A	Given

Table 6 Output parameters from electromagnetic design calculations

Output parameter	**Calculated value**	**Unit**	**Calculation**
Turns density, $n = N/L$	11,500	turns/m	1150 / 0.10
Calculated magnetic flux density, B	≈ 11.55	T	$\mu_0 K n I$
Calculated electromagnetic force, F	≈ 4.62	N	$B I L$

8.1 Solenoid magnetic-field calculation

For the magnetic-field estimate, the project uses the solenoid relation $B = \mu nI$, where $\mu = K\mu_0$ and $n = N/L$. The values are $K = 200$, $N = 1150$ turns, $L = 0.1$ m and $I = 4$ A. The resulting turns density and magnetic flux density are calculated below. These calculations are numbered Eq. 1, Eq. 2 and Eq. 3.

$$n = N/L = 1150/0.1 = 11{,}500 \text{ turns/m} \quad (1)$$

$$\mu = K\,\mu_0 = 200 \times 4\pi \times 10^{-7} \text{ H/m} \quad (2)$$

$$B = \mu n I \approx 11.55\ \text{T} \quad (3)$$

Using L = 0.1 m, the project applies F = BIL and obtains 4.62 N. This value is retained because it is the force reported in the source calculation. In a practical electromagnetic actuator, however, force also depends on coil geometry, the magnetic circuit, air gap, saturation and the actual field distribution. The reported 4.62 N should therefore be treated as a preliminary estimate and verified experimentally or with electromagnetic finite-element analysis. Published actuator design studies also consider thermal and volume constraints (Gysen *et al.*, 2009). Table 7 summarises these electromagnetic quantities.

Table 7 Summary of reported electromagnetic actuator quantities

Quantity	**Symbol**	**Value reported/used**
Relative permeability	*K*	200
Number of turns	*N*	1150
Coil length	*L*	0.1 m
Turns per metre	*n*	11,500 turns/m
Current	*I*	4 A DC
Calculated magnetic flux density	*B*	≈11.55 T
Reported force calculation	*F*	4.62 N

8.2 Structural-load consistency note

The original report also associates the 783.96 N load with approximately 7690 kg. These quantities are not dimensionally consistent when the load is treated as an equivalent gravitational force: 783.96 N corresponds to about 79.9 kgf at 9.81 m/s^2. The original simulation setup should therefore be checked before the 7690 kg value is used in a publication or design certification. The reported displacement values have been retained as given.

Fig. 1–8 document the proposed suspension architecture, vehicle-representative geometry, CAD configurations and fabricated test rig. Fig. 9–12 present the theoretical electromagnetic trends and the reported structural-displacement comparison used for the preliminary assessment.

9. Results and discussion

The plots in this section illustrate the calculated effect of selected input quantities on the reported outputs. The current–field and current–force curves are obtained from the equations and parameters given in the project report; they are theoretical trends rather than new experimental measurements. The structural comparison uses the reported displacements for the 783.96 N load case. In contrast to these calculated trends, the published direct-drive study in (Gysen *et al.*, 2011) used quarter-car measurements to validate its analysis and simulations. Thus, the present curves do not establish validated dynamic or energy-recovery performance. The calculated trends and structural comparison are shown in Fig. 9, Fig. 10, Fig. 11 and Fig. 12. Table 8 summarises the principal results.

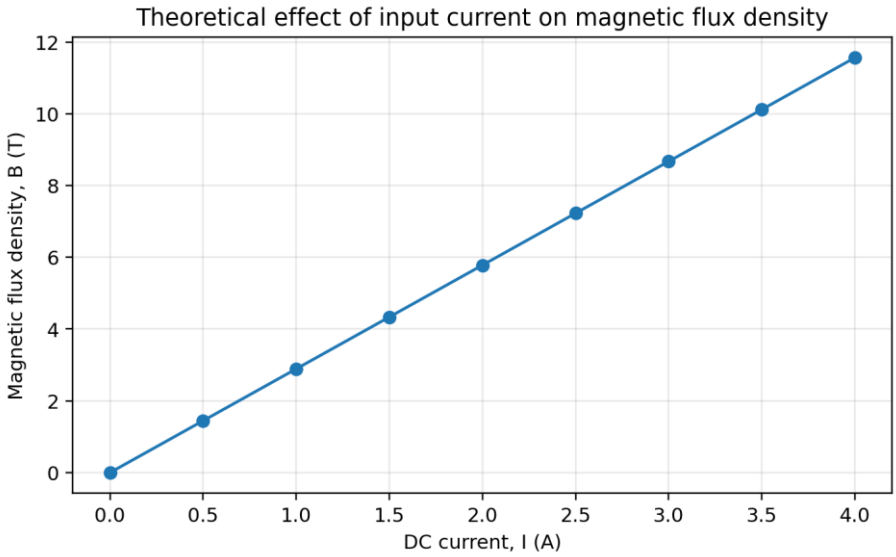


Fig. 9 Theoretical relationship between DC current and magnetic flux density (N = 1150, L = 0.10 m, K = 200); calculated from the project-report equations and inputs.

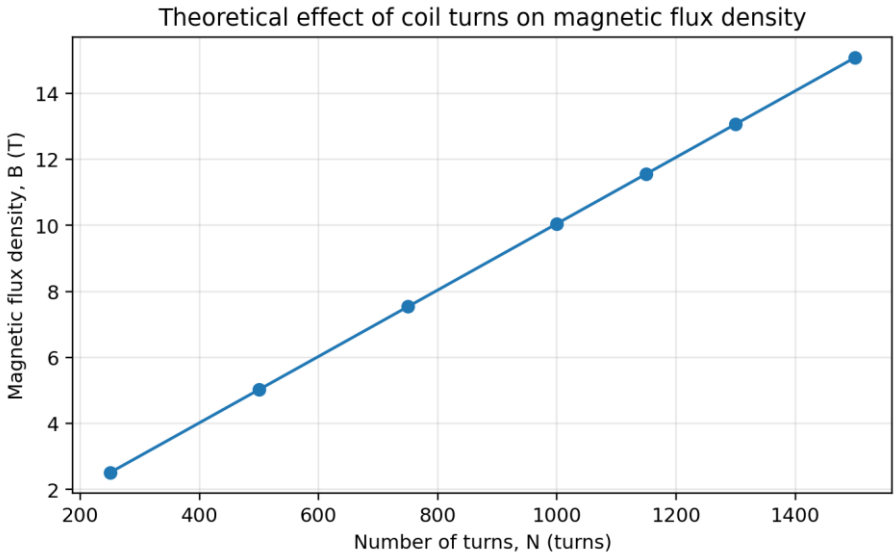


Fig. 10 Theoretical relationship between number of coil turns and magnetic flux density (I = 4 A, L = 0.10 m, K = 200); calculated from the project-report equations and inputs.

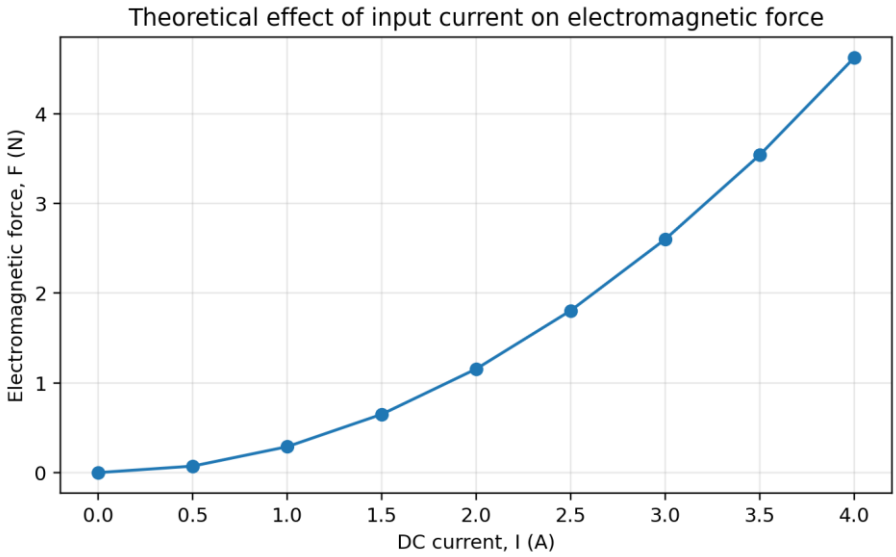


Fig. 11 Theoretical relationship between DC current and electromagnetic force using the force equation; calculated from the project-report equations and inputs.

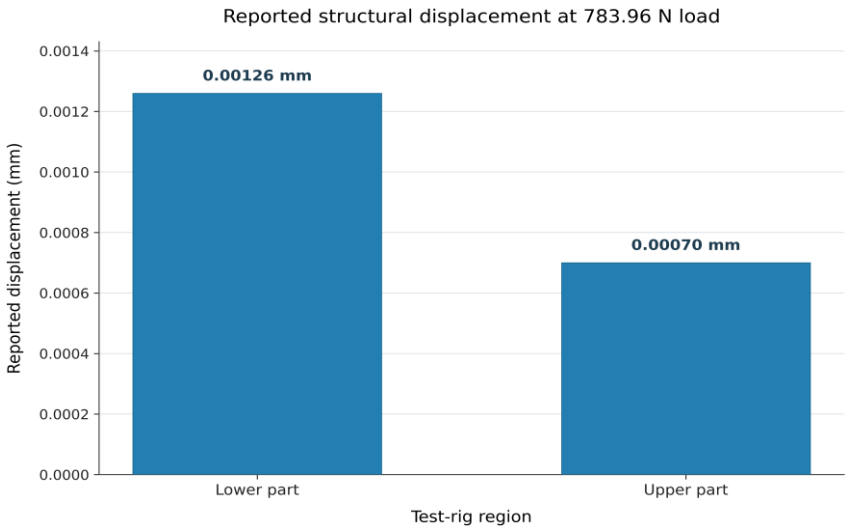


Fig. 12 Comparison of reported structural displacement of the lower and upper test-rig sections at 783.96 N; structural results from the present study.

Table 8 Principal results and engineering significance of the fabricated test rig

Result / observation	**Source evidence**	**Engineering significance**
Second test-rig design selected	Simpler, safer and lower material requirement	Improves manufacturability and laboratory safety.
Structural load analysed	783.96 N	Provides preliminary verification of structural response.
Lower displacement	0.00126 mm	Small modelled deformation.
Upper displacement	0.0007 mm	Small modelled deformation.
Fabricated assembly	Spring, damper and electromagnetic system fitted	Demonstrates physical integration.
Functional movement	Reported as successful	Confirms basic mechanical operation.

10. Outcomes of the study

- At N = 1150 turns, L = 0.10 m, K = 200 and I = 4 A, the reported calculation gives a magnetic flux density of approximately 11.55 T.

- The turns density calculated from $n = N/L$ is 11,500 turns/m.
- For I = 0–4 A, the calculated magnetic flux density increases from 0 to about 11.55 T. At 1, 2, 3 and 4 A, the calculated values are approximately 2.89, 5.78, 8.66 and 11.55 T, respectively.
- With N, L and K held constant, each 1 A increase in current raises the calculated magnetic flux density by about 2.89 T.
- At I = 4 A and L = 0.10 m, increasing the number of turns increases the calculated magnetic flux density. For 250, 500, 750, 1000, 1150, 1300 and 1500 turns, the calculated values are approximately 2.51, 5.03, 7.54, 10.05, 11.56, 13.06 and 15.08 T, respectively.
- Increasing the number of turns from 250 to 1500 raises the calculated magnetic flux density by about 12.57 T, or roughly five times the value at 250 turns, with the other inputs unchanged.
- From the reported relation F = BIL, the calculated electromagnetic force at B = 11.55 T, I = 4 A and L = 0.10 m is approximately 4.62 N.
- Using the same equation, the calculated force at I = 1, 2, 3 and 4 A is approximately 0.29, 1.16, 2.60 and 4.62 N, respectively.
- From 1 A to 4 A, the calculated force increases by about 4.33 N, corresponding to approximately 1500 % according to the source-based calculation.
- Structural analysis of the selected second test-rig design was carried out for the reported applied load of 783.96 N.
- The reported displacement is 0.00126 mm for the lower section and 0.00070 mm for the upper section.
- The lower-section displacement is 0.00056 mm greater than the upper-section value and is about 1.80 times the upper value.
- Both reported displacement values are below 0.002 mm, indicating very small calculated deformation for the stated load case.
- The reported small displacements supported the selection of the second test-rig design for fabrication. The fabricated rig used 3 mm mild steel.
- The fabricated test rig accommodated the spring, damper and retrofit electromagnetic system, and its movement was reported to be satisfactory during the practical check.
- The work demonstrates that an electromagnetic suspension arrangement can be fabricated and examined at laboratory/test-rig scale.
- The proposed arrangement combines electromagnetic or permanent-magnet forces with conventional spring and damping components, allowing electromagnetic assistance without completely replacing the existing suspension arrangement.
- The retrofit configuration was intended to allow integration with an existing vehicle suspension with limited modification.
- A CAD-based test rig was developed from dimensions measured on an actual vehicle suspension. Two designs were prepared, and the second was selected because of its simpler fabrication, lower material requirement and protective cover.
- The final rig was fabricated by cutting, shearing, bending and welding the structural members, followed by installation of the spring, damper and electromagnetic subsystem.
- The electromagnetic results are calculated trends obtained from the equations and parameters in the source report. They should not be treated as experimentally measured current–field or current–force data.
- The reported electromagnetic force is a preliminary design estimate and needs experimental force measurement or dedicated electromagnetic simulation for validation.
- The structural assessment is also preliminary because complete stress values, mesh details, material properties, boundary conditions, factor of safety and convergence information are not available in the source material.
- Important performance measures such as transmissibility, acceleration response, damping coefficient, force versus displacement, harvested energy, electrical power, temperature rise and ride-comfort indices were not reported and require further testing.

- Further work can examine coil turns, permanent-magnet selection, vibration and displacement sensing, closed-loop control, lightweight construction and electromagnetic finite-element analysis.

11. Limitations and future work

- Investigate how coil turns and current affect electromagnetic force and suspension stiffness.
- Use high-performance neodymium permanent magnets where appropriate to increase magnetic force within a compact arrangement.
- Replace PVC structural elements with carbon-fibre or other lightweight materials where suitable.
- Add vibration, displacement, infrared or other sensors for real-time measurement of suspension motion and condition.
- Develop closed-loop control using gap or displacement feedback with a microcontroller or digital signal processor (DSP) (Fu *et al.*, 2023).
- Measure transmissibility, acceleration, damping force, electromagnetic force and ride response under controlled excitation (Gysen *et al.*, 2009; Gysen *et al.*, 2011).
- Assess regenerative operation by measuring voltage, current, power and energy generated during each suspension cycle (Gysen *et al.*, 2011).
- Carry out electromagnetic finite-element analysis to study air-gap effects, saturation, force–displacement behaviour and thermal response.
- Conduct fatigue, durability and vehicle-level road tests before considering practical automotive deployment.
- Optimise the system for lower mass, compact packaging, reduced power consumption and improved thermal management (Gysen *et al.*, 2009; Fu *et al.*, 2023; Puliti *et al.*, 2024).

12. Conclusion

A practical electromagnetic suspension concept and a corresponding test rig were developed from the research work. The arrangement combines electromagnetic or permanent-magnet force with conventional spring and damping elements, providing an additional controllable function without completely replacing the existing suspension layout.

Dimensions measured from a real vehicle suspension were used for CAD development. Two test-rig configurations were prepared, and the second was selected because it simplified fabrication and included a protective upper cover. The final rig was manufactured from 3 mm mild steel using cutting, shearing, bending and welding processes. The spring, damper and retrofit electromagnetic subsystem were then integrated into the structure.

For the reported 783.96 N structural load, the calculated displacements were 0.00126 mm and 0.0007 mm for the lower and upper sections, respectively. The electromagnetic calculation gave approximately 11.55 T and 4.62 N using the simplified equations and parameters specified in the source. These values indicate preliminary feasibility of the test-rig concept, but further experimental and numerical work is required before conclusions can be extended to complete automotive suspension performance.

Acknowledgement

The authors sincerely acknowledge the support and guidance provided by the Department of Mechanical and Production Engineering.

References

Abdelkareem, M. A. A., Xu, L., Ali, M. K. A., Elagouz, A., Mi, J., Guo, S., Liu, Y., & Zuo, L. (2018). Vibration energy harvesting in automotive suspension system: A detailed review. Applied Energy, 229, 672–699. https://doi.org/10.1016/j.apenergy.2018.08.030

Bose Corporation. (2011). Bose active suspension system. [URL not provided].

Dahat, N., Maskar, P., & Yadav, A. (2023). Design and development of regenerative shock absorber. Materials Today: Proceedings, 82, 363–368. https://doi.org/10.1016/j.matpr.2023.02.433

Danby, G., & Powell, J. (1966). Electrodynamic suspension/null-flux concept. [Complete publication details not available].

Ding, R., Chen, X., Wang, R., & Jiang, D. (2026). A review of configurations and control strategies for linear motor-based electromagnetic suspension. Machines, 14(1), Article 2. https://doi.org/10.3390/machines14010002

Fu, C., Lu, J., Ge, W., Tan, C., & Li, B. (2023). A review of electromagnetic energy regenerative suspension system & key technologies. Computer Modeling in Engineering & Sciences, 135(3), 1779–1824. https://doi.org/10.32604/cmes.2022.023092

Gysen, B. L. J., Janssen, J. L. G., Paulides, J. J. H., & Lomonova, E. A. (2009). Design aspects of an active electromagnetic suspension system for automotive applications. IEEE Transactions on Industry Applications, 45(5), 1589–1597. https://doi.org/10.1109/TIA.2009.2027097

Gysen, B. L. J., Paulides, J., Janssen, J., & Lomonova, E. (2010). Active electromagnetic suspension system for improved vehicle dynamics. IEEE Transactions on Vehicular Technology, 59, 1156–1163. https://doi.org/10.1109/TVT.2009.2038706

Gysen, B. L. J., van der Sande, T. P. J., Paulides, J. J. H., & Lomonova, E. A. (2011). Efficiency of a regenerative direct-drive electromagnetic active suspension. IEEE Transactions on Vehicular Technology, 60(4), 1384–1393. https://doi.org/10.1109/TVT.2011.2131160

Lauwerys, C., Swevers, J., & Sas, P. (2005). Robust linear control of an active suspension on a quarter car test-rig. Control Engineering Practice, 13, 577–586.

Li, Z., Zuo, L., Luhrs, G., Lin, L., & Qin, Y.-X. (2013). Electromagnetic energy-harvesting shock absorbers: Design, modeling, and road tests. IEEE Transactions on Vehicular Technology, 62(3), 1065–1074. https://doi.org/10.1109/TVT.2012.2229308

Liu, P., Kou, F., Chen, Y., Wang, G., Lv, W., & Xing, L. (2025). A novel hybrid electromagnetic-hydraulically interconnected actuator suspension: Dynamic modeling, bench test and ride analysis. Mechanical Systems and Signal Processing, 236, Article 113028. https://doi.org/10.1016/j.ymssp.2025.113028

Lu, J., Wu, H., Li, B., Fu, C., Tan, C., Wei, W., Sun, B., & Xie, X. (2025). Optimal design of an integrated electromagnetic linear energy regenerative suspension system based on a hybrid optimization objective. Energy, 327, Article 136176. https://doi.org/10.1016/j.energy.2025.136176

Martins, I., Esteves, J., Marques, G. D., & da Silva, F. P. (2006). Permanent-magnets linear actuators applicability in automobile active suspensions. IEEE Transactions on Vehicular Technology, 55(1), 86–94. https://doi.org/10.1109/TVT.2005.861167

Paulides, J. J. H., Encica, L., Lomonova, E. A., & Vandenput, A. J. A. (2006). Design considerations for a semi-active electromagnetic suspension system. IEEE Transactions on Magnetics, 42(10), 3446–3448. https://doi.org/10.1109/TMAG.2006.879963

Puliti, M., Galluzzi, R., Tessari, F., Amati, N., & Tonoli, A. (2024). Energy efficient design of regenerative shock absorbers for automotive suspensions: A multi-objective optimization framework. Applied Energy, 358, Article 122542. https://doi.org/10.1016/j.apenergy.2023.122542

Sharkawy, A. (2005). Fuzzy and adaptive fuzzy control for the automobiles active suspension system. Vehicle System Dynamics, 43(11), 795–806.

Shi, X., Yu, Q., Wu, Z., Li, J.-Y., & Zhu, S. (2024). Active control for vehicle suspension using a self-powered dual-function active electromagnetic damper. Journal of Sound and Vibration, 569, Article 117976. https://doi.org/10.1016/j.jsv.2023.117976

Sun, D., Ding, R., & Dong, R. (2025). A review of linear motor electromagnetic energy regenerative suspension and key technologies. Energies, 18(19), Article 5158. https://doi.org/10.3390/en18195158

Tulsian, N., & Dewangan, S. (2023). A discussion on energy harvesting through suspension system. Materials Today: Proceedings, 79(Part 2), 189–192. https://doi.org/10.1016/j.matpr.2022.10.052

Wang, J., A. K., & H. D. (2008). Comparative studies of linear permanent magnet motor topologies for active vehicle suspension. In 2008 IEEE Vehicle Power and Propulsion Conference (pp. 1–6). [Complete author and publication details require verification].

Wu, K., Ren, C., & Atay, F. M. (2024). Enhancing energy recovery in automotive suspension systems by utilizing time-delay. Energy, 300, Article 131578. https://doi.org/10.1016/j.energy.2024.131578

Xing, L., Kou, F., Wang, G., Liu, P., Lv, W., & Yang, C. (2025). Energy recovery and energy-saving control of a novel hybrid electromagnetic active suspension system for electric vehicles. Energy, 335, Article 138030. https://doi.org/10.1016/j.energy.2025.138030

Xiong, X., Liu, C., Fan, L., & Xu, F. (2025). Design and performance analysis of an energy harvesting suspension system utilizing Halbach-like permanent magnet arrays. Proceedings of the Institution of Mechanical Engineers, Part D: Journal of Automobile Engineering, 239(10–11). https://doi.org/10.1177/09544070241272907

Yang, Y.-G., & Cen, M.-H. (2024). Stochastic dynamics of an electromagnetic energy harvesting suspension with time-delayed feedback and fractional damping. International Journal of Non-Linear Mechanics, 165, Article 104766. https://doi.org/10.1016/j.ijnonlinmec.2024.104766

Zhang, R., Zhao, L., Qiu, X., Zhang, H., et al. (2020). A comprehensive comparison of the vehicle vibration energy harvesting abilities of the regenerative shock absorbers predicted by the quarter, half and full vehicle suspension system models. Applied Energy, 272, Article 115180. https://doi.org/10.1016/j.apenergy.2020.115180

Zuo, L., Scully, B., Shestani, J., & Zhou, Y. (2010). Design and characterization of an electromagnetic energy harvester for vehicle suspensions. Smart Materials and Structures, 19(4), Article 045003. https://doi.org/10.1088/0964-1726/19/4/045003